



HAL
open science

Heparan sulphate 6-O-endosulphatases: discrete in vivo activities and functional co-operativity

William C Lamanna, Rebecca J Baldwin, Michael Padva, Ina Kalus, Gerdy ten Dam, Toin H van Kuppevelt, John T Gallagher, Kurt von Figura, Thomas Dierks, Catherine Lr Merry

► To cite this version:

William C Lamanna, Rebecca J Baldwin, Michael Padva, Ina Kalus, Gerdy ten Dam, et al.. Heparan sulphate 6-O-endosulphatases: discrete in vivo activities and functional co-operativity. *Biochemical Journal*, 2006, 400 (1), pp.63-73. 10.1042/BJ20060848 . hal-00478612

HAL Id: hal-00478612

<https://hal.science/hal-00478612>

Submitted on 30 Apr 2010

HAL is a multi-disciplinary open access archive for the deposit and dissemination of scientific research documents, whether they are published or not. The documents may come from teaching and research institutions in France or abroad, or from public or private research centers.

L'archive ouverte pluridisciplinaire **HAL**, est destinée au dépôt et à la diffusion de documents scientifiques de niveau recherche, publiés ou non, émanant des établissements d'enseignement et de recherche français ou étrangers, des laboratoires publics ou privés.

HEPARAN SULPHATE 6-O-ENDOSULPHATASES–

DISCRETE *IN VIVO* ACTIVITIES AND FUNCTIONAL COOPERATIVITY

William C. Lamanna^{*,‡,1}, Rebecca J. Baldwin^{†,1}, Michael Padva[‡], Ina Kalus^{*}, Gerdy ten Dam[§], Toin H. van Kuppevelt[§], John T. Gallagher[†], Kurt von Figura[‡], Thomas Dierks^{*,¶}, Catherine L. R. Merry^{†,¶}

From the ^{*}Dept. of Chemistry, Biochemistry I, Bielefeld University, Universitätsstr. 25, 33615 Bielefeld, Germany; [†]University of Manchester and Cancer Research UK Department of Medical Oncology, Christie Hospital NHS Trust, Manchester, UK; [‡]Dept. of Biochemistry II, University of Goettingen, Heinrich-Düker-Weg 12, 37073 Goettingen, Germany; [§]Dept. Biochemistry 280, Nijmegen Center for Molecular Life Sciences, Radboud University Nijmegen Medical Centre, PO Box 9101, 6500 HB Nijmegen, The Netherlands; [¶]Current address: School of Materials, Materials Science Centre, The University of Manchester, Manchester, UK.

¹These authors contributed equally to this work

Running title: Molecular phenotype of mSulf1 and mSulf2 knock out

¶Address correspondence to: catherine.merry@manchester.ac.uk; Tel: +44 (0)161 306 8871, Fax: +44 (0)161 306 8877 and thomas.dierks@uni-bielefeld.de; Tel: +49 (0)521 106 2092, Fax: +49 (0)521 106 6014

Keywords: glycosaminoglycans/heparan sulphate/knock out mice/signal transduction/sulphatases

Heparan sulphate (HS) is essential for normal embryonic development. This requirement is due to the obligatory role for HS in the signalling pathways of many growth factors and morphogens that bind to sulphated domains in the HS polymer chain. The sulphation patterning of HS is determined by a complex interplay of Golgi-located N- and O-sulphotransferases that sulphate the heparan precursor and cell surface endosulphatases that selectively remove 6-O-sulphates (6S) from mature HS chains. In the present study we generated single or dual knock out mice for the two murine endosulphatases mSulf1 and mSulf2. Detailed structural analysis of HS from *mSulf1*^{-/-} fibroblasts showed a striking increase in 6-O-sulphation, which was not seen in *mSulf2*^{-/-} HS. Intriguingly, the level of 6-sulphation in the double *mSulf1*^{-/-}/*mSulf2*^{-/-} HS was significantly higher than that in the *mSulf1*^{-/-} counterpart. These data imply that mSulf1 and mSulf2 are functionally cooperative. Unlike their avian orthologues, mammalian Sulf activities are not restricted to the highly sulphated S-domains of HS. Mitogenesis assays with FGF2 revealed that Sulf activity dampens the activating potential of newly-synthesised HS suggesting an important role for these enzymes in cell growth regulation in embryonic and adult tissues.

Heparan sulphate proteoglycans (HSPGs) are some of the most abundant proteins on the cell surface and within the extracellular matrix. The sulphate groups on the HS chains of these glycoconjugates form specific patterns which direct key aspects of cell growth, differentiation, adhesion and migration by regulating the interaction of growth factors with their cognate receptors and by modulating transport and diffusion of many growth and morphogenic factors [1]. For some ligands such as members of the fibroblast growth factor (FGF) family, the interaction with specific sulphate patterns is essential for signalling [2, 3]. Sulphate pattern regulation therefore plays a critical role during development and disease pathogenesis.

Within a mature HS chain (typically between 50 and 200 saccharides in length) long sequences of repeating GlcA-GlcNAc residues are separated by composite regions consisting of highly sulphated S-domains (predominantly IdoA(2S)-GlcNS sequences) with adjacent transition zones comprised of alternating GlcNS and GlcNAc containing disaccharides [4]. Both the S-domains and transition zones are further modified by 6-O-sulphation (6S) of glucosamine residues and variations in the degree and patterning of 6S contribute significantly to the fine structural heterogeneity in HS. The structural diversity in HS is non-random, with regulation observed at the level of tissue type and developmental stage [5, 6]. Within the specific domain types loss or gain of 6S alone is sufficient to alter the outcome of the ligand-HS interaction [7].

Dynamic changes in 6S correlate with modulated susceptibility to FGF signal transduction during neural development and tumour transformation [8, 9].

The regulation of 6S patterning was thought to be solely the result of the action of the HS biosynthetic enzymes; however the identification of the Sulfs, a family of HS endo-6-O-sulphatases, has led to a revision of this viewpoint. The first Sulf was discovered in a molecular cloning screen for Sonic hedgehog responsive genes, which led to the characterization of QSulf1, a sulphatase regulating cellular differentiation through modulation of Wnt signalling in developing quail embryos [10]. Orthologues were identified in mammalian species [11], however, many of the insights into Sulf activity have come from studies using QSulf1 and its recently characterized isoform QSulf2 [12-15]. The unique localisation of the Sulfs at the cell surface and their endolytic activity, rather than the exolytic and therefore catabolic activity of lysosomal sulphatases, carried with it important implications for the novel hydrophilic domain that is inserted into the catalytic domain of the Sulfs. This highly and mainly positively charged domain has recently been characterised as a decisive functional element for both substrate recognition and cell surface localisation [12]. The native substrate specificity of the Sulfs has, until now, been largely studied employing HS disaccharide analysis from QSulf over-expressing cellular systems or *in vitro* analysis [12, 13]. Results from these experiments indicate a substrate specificity of QSulf1 and QSulf2 which is completely restricted to GlcA/IdoA(2S)-GlcNS(6S) type disaccharides from the S-domains of HS [12-14].

Attention has now turned to the mammalian Sulf orthologues in mice and humans, as both Sulf1 and 2 isoforms have been shown to be mis-regulated during mammalian tumourigenesis [16-18]. Investigations into the influence of Sulf activity on HS-binding factors active in tumourigenesis such as VEGF, FGF, HGF and HB-EGF [19-21] have led to the hypothesis that the modulation of Sulf activity may be a target for therapeutic intervention.

In this study we describe the first characterisation of HS produced by cells with a knock out for mSulf1, mSulf2 or both. We have combined detailed structural analysis of the HS with expression analyses, HS epitope characterisation and growth factor activity studies. We conclude that mSulf1 and mSulf2 show functional cooperativity and that although increased mSulf1 expression can compensate for loss of mSulf2 activity, mSulf2 is unable to fulfil the role of mSulf1. Importantly, the 6-O-desulphation catalysed by the mSulf enzymes was found to be extensive, and more widely distributed throughout the HS chain than observed with the QSulf orthologues, with significant implications for the range of HS-ligand interactions affected.

Finally, the use of a panel of ScFv antibodies to characterise mSulf-mediated changes in HS structure suggest a novel method for the *in vivo* detection of aberrant mSulf activity.

EXPERIMENTAL PROCEDURES

Materials - Dulbecco's modified Eagle's medium and foetal calf serum were from Life Technologies, Inc. Heparinase I-III (*Flavobacterium heparinum*) were all from Grampian Enzymes (Orkney, UK). Chondroitinase ABC (*Proteus vulgaris*) and monoclonal antibodies against diphosphorylated ERK1/2 were from Sigma. The gels used were Sepharose CL-6B and DEAE-Sepharcel (GE Healthcare) and Bio-Gels P-10 (fine grade) and P-2 (Bio-Rad). The ProPac PA-1 HPLC column was from Dionex (Camberley, UK). D-[6-³H]glucosamine hydrochloride (20-45 Ci mmol⁻¹) and Na₂³⁵SO₄ (1050-1600 Ci mmol⁻¹) were from GE Healthcare and Perkin Elmer Life Sciences, respectively. Recombinant human FGF2, and HGF/SF were from R&D Systems (Abingdon, UK).

Generation of knock out mice, genotyping and Northern analysis - By screening a genomic cosmid library of the 129Sv/Ola mouse (German Resource Center for Genome Research, Berlin) with labelled cDNA fragments as probes, cosmids were identified that carried fragments of the *mSulf1* or *mSulf2* gene. A 3.1 kb HindIII fragment carrying exon 2 of *mSulf1* and a 3.8 kb Sall/EcoRI fragment carrying exon 1 of *mSulf2* with about equal homology arms of 1.5-2.0 kb on both sides (Figure 1 A/B) were sequenced, subcloned into pBluescriptII SK and used for construction of the targeting vectors. The neomycin resistance cassette, a blunted XhoI/Sall fragment of the pMC1neo vector (Stratagene), was inserted into the BsaAI site of *mSulf1* exon 2 as well as into the blunted BseRI site of *mSulf2* exon 1 (Figure 1 A/B), thereby disrupting the respective reading frames and generating stop codons in all frames. NotI-linearized constructs were electroporated into 129Sv/Ola embryonic stem cells (cell line D3, kindly provided by Peter Gruss, Goettingen). G418-resistant clones were selected and genotyped for specific recombination by Southern blotting. Positive ES clones were injected into C57BL/6 blastocysts to produce chimeric mice. Male chimeras were mated with C57BL/6 females, which led to germ line transmission of the targeted alleles. From these, heterozygotes were intercrossed to generate wild type and knock out mice. Northern and Southern blotting was performed according to standard methods using PCR-generated probes (primers listed in Supplementary Table I). The *mSulf2* 5'-external probe was a 420 bp EcoRI/HindIII fragment of EST clone IMAGp998G091033Q2 (German Resource Center for Genome Research, Berlin).

Preparation of HS from MEF cultures - Embryos (E12.5) obtained from mating *mSulf1*^{-/-}, *2*^{-/-} or *mSulf1*^{-/-}/*mSulf2*^{+/-} mice were dissected, MEFs isolated and the HS chains radiolabelled and

purified as described previously [22]. Primary MEFs from the *mSulf1*^{-/-}/*2*^{-/-} embryos could not be maintained in culture. We therefore prepared immortalised lines (*mSulf1*^{-/-}/*2*^{-/-} and wild type control) by stable transfection of MEFs (E12.5) with the pMSSVLT vector containing an SV40 fragment including the large T gene [23], prior to isolation of HS chains.

Disaccharide compositional analysis - HS chains (50 Kcpm of ³H) were digested with a combination of heparinases I, II, and III and the resultant disaccharides identified following SAX-HPLC as described previously [22].

Low pH nitrous acid depolymerisation - 100 Kcpm (³H) of HS was taken for low pH nitrous acid depolymerisation [22]. Oligosaccharides produced were separated and the tetrasaccharides purified essentially as described by Viviano et al. [14]. Recovered tetrasaccharides were then separated by SAX-HPLC as for the heparinase I/II/III generated disaccharides.

Heparinase III digestion - 100 Kcpm (³H) of HS was treated with heparinase III essentially as described by Merry et al. [24]. Isolated sized fragments were pooled, desalted and further fractionated by SAX-HPLC. Disaccharides were analysed as described for heparinase I/II/III generated disaccharides. For larger oligosaccharides a single ProPac PA-1 SAX column was used with a linear gradient running from 0-0.75 M NaCl over 110min. Peak identification was made by comparison with previously published profiles [24].

Real Time PCR - Primary wild type, *mSulf1*^{-/-} and *mSulf2*^{-/-} MEFs together with immortalised wild type and *mSulf1*^{-/-}/*2*^{-/-} MEFs were washed in PBS then harvested. RNA was extracted using the RNeasy Protect mini kit (Qiagen, 74124). Synthesis of cDNA from mRNA transcripts was performed using the following method: RNA (5µg, denatured at 65°C for 3 minutes and placed on ice), dNTP (250µM), oligo dT (5µg; Promega, UK), 1X AMV buffer (Promega) and AMV reverse transcriptase (40 units; Promega) in a total volume of 200µl was incubated at 42°C for 1 hour, followed by 98°C for 5 minutes. Real time PCR assays to the Sulf enzymes together with housekeeping genes L19 and EEF1G were designed using the Exiqon Mouse Universal Probe Library system [25]; (www.universalprobelibrary.com) (Roche, Switzerland), with amplification primers obtained from MWG (Germany). Amplicons were designed to be intron-spanning typically between 60-100 nucleotides in length. Real time PCR reactions were set up using SensiMix (dT) (Quantace) as per instructions. Briefly for a 10µl reaction, 5ng of cDNA, 0.1µM each forward and reverse primer, 0.1µl of the appropriate mouse probe (Universal ProbeLibrary Set, Roche applied science), 5 µl reaction buffer and water up to 10 µl was mixed per well of a 384 well clear optical reaction plate (ABgene). Each primer/cDNA set was set up in triplicate

and the whole experiment was repeated three times. For primer/probe combinations see Supplementary Table II. Experiments were performed on an ABI 7900 Real Time Sequence Detection System, using an Epmotion 5070 robot (Eppendorf, Germany) for plate set up. Assays were tested for efficiency using reference RNA and a 10 fold dilution series; only assays with greater than 99% amplification efficiency were used for subsequent work. Data analysis was performed using the $\Delta\Delta C_t$ method [26], normalising against L19 and EEF1G allowing the fold change relative to wild type to be calculated.

FACS analysis: 96 well plate format - Cells were harvested using dissociation buffer and resuspended in PBS. Cells were distributed at 1×10^6 cells/well in a round-bottom 96-well plate and fixed in 1% formaldehyde, 4°C for 15 minutes prior to staining. Cells were then washed in PBS and resuspended in 100 μ l FACS buffer (0.2% BSA, 0.1% sodium azide in PBS) containing primary ScFv antibody (HS4C3, RB4EA-12, AOB408, HS4E4, EV3C3 and MPB49V (control), periplasmic fractions 1/10), incubating at 4°C for 1 hour. Cells were washed twice with 100 μ l PBS and resuspended in 100 μ l FACS buffer containing anti-mouse VSV (1/1000, Sigma, V-5507), incubating at 4°C for 45 minutes. Cells were then washed twice in PBS. Tertiary antibody goat anti-mouse IgG-PE (1/100, molecular probes, P-852) was then added in 100 μ l FACS buffer and incubated at 4°C for 45 minutes. Cells were then washed twice in PBS and fixed in 1% formaldehyde, and transferred to a FACS tube (Falcon, 352054). Control cells were incubated as above omitting the primary antibody step. Cell fluorescence was measured in a Becton Dickinson FACScan. Viable cells were gated using forward and side scatter, and the fluorescence of this population was measured.

Mitogenesis assay - A simple mitogenesis assay was established using wild type and knock out primary MEFs. Cells were plated at 25,000 cells per well on a 24-well plate in 1ml of serum free DMEM. After incubating for 4 hours at 37°C, HGF or FGF2 was added at 10ng/ml. Cells were subsequently incubated at 37°C for 36 hours before being counted manually under a light microscope in 15 individual fields per well. The average number of cells per well was calculated and the fold increase/decrease was determined by comparing the average number of cells per well in growth factor induced and untreated control cells.

RESULTS AND DISCUSSION

An essential function of HS is to provide a scaffold on the cell surface for mediating the interaction of signalling molecules, whereby the sulphation patterns of HS largely determine ligand binding affinities. The endo-sulphatases Sulf1 and Sulf2 act as key players in sulphation pattern remodelling. To investigate the role of these enzymes *in vivo*, *mSulf1* and *mSulf2* knock out mice were generated.

Phenotypic characterisation - *mSulf1* and *mSulf2* knock out mice were generated by the classical approach, i.e. by insertion of a neomycin resistance cassette into exon 2 of the murine *Sulf1* gene and exon 1 of the murine *Sulf2* gene, as outlined in Figure 1A/B. Northern analysis of mRNA from knock out mouse embryonic fibroblasts (MEFs) verified the absence of wild type *mSulf1* or *mSulf2* transcripts, respectively (Figure 1C). By real-time PCR very low amounts of targeted, i.e. non-functional, transcripts could be detected (see below). *mSulf1*^{-/-} mice show no obvious phenotype. However, their mortality in the first month of life was slightly, but consistently increased. *mSulf2*^{-/-} mice show a small reduction in litter size and body weight. Their mortality within the first 6 weeks was increased. Death of the *mSulf2*^{-/-} mice was usually associated with malformations, in particular of the brain (I. Kalus et al., in preparation). Survivors appear normal. Double knock out animals were difficult to obtain. After many heterozygous matings we obtained very few fertile *mSulf1*^{-/-}/*2*^{-/-} animals, which were used for homozygous matings. In this way we recently succeeded to obtain five litters with a ≈2-fold reduced size (4.4±0.9 animals). These animals typically have a very short life span and a clear reduction in body weight. Double knock out MEFs could be obtained from E12.5 embryos and are described below.

The knock out approach is distinct from those which have previously investigated the function of the Sulf enzymes in that we are interpreting Sulf activity from the effects of its loss, as opposed to the over-expression studies frequently used, or the *in vitro* recapitulations of activity using isolated enzyme fractions. We believe this strategy is more biologically significant, as the amount and sub-cellular localisation of all the other components of the HS biosynthetic and modification machinery are maintained and thus are only influenced by the loss of Sulf activity.

Therefore the interplay between these factors and the Sulf enzymes is likely to be more representative of their true *in vivo* activity.

Molecular Phenotype: Effect on HS disaccharide composition and overall sulphation - As stated earlier, HS structure is tissue specific; however, it has previously been demonstrated that the loss/mutation of HS biosynthetic enzymes in a knock out model has a similar effect on all tissues [5, 22]. We therefore chose MEFs as a convenient source of material for detailed structural analyses. Metabolically $^3\text{H}/^{35}\text{S}$ -radiolabelled HS was purified from primary wild type, *mSulf1*^{-/-} and *mSulf2*^{-/-} MEFs as well as from immortalised *mSulf1*^{-/-}/*2*^{-/-} and wild type MEFs. Immortalisation was necessary as it proved impossible to maintain the *mSulf1*^{-/-}/*2*^{-/-} MEFs in culture for long enough to allow the preparation of radiolabelled HS. HS from all cells was digested with a combination of heparinases I, II and III and the resultant disaccharides resolved on a Bio-Gel P2 column. The disaccharides were then pooled and fractionated by SAX-HPLC (Table 1 and Supplementary Figure 1). Significant increases were observed in all 6S disaccharide species in the *mSulf1*^{-/-} HS compared with the wild type HS (Table 1). No overall increase in 6S was observed in the *mSulf2*^{-/-} HS although there was a significant increase in the UA-GlcNAc(6S) disaccharide unit known to be associated with transition zones (see below). The *mSulf1*^{-/-}/*2*^{-/-} HS showed large increases in all 6S disaccharides. Comparing the relative abundance of 6S disaccharides between single and double knock out cells revealed a greater than two fold increase of S-domain associated disaccharides, UA-GlcNS(6S) and UA(2S)-GlcNS(6S), in the double knock out HS as compared to either single knock out HS, thus indicating cooperativity between the two Sulf activities within the S-domains (Table 1).

Interestingly, the increase in 6S in the mSulf knock out cells was accompanied by small but statistically significant reductions in other sulphation events, particularly in the level of 2S (Table 1 and Supplementary Figure 1). It is therefore important to apply caution to the interpretation of experiments where loss (or gain) of Sulf activity influences HS-ligand interactions, as these may not necessarily be due to changes in 6S alone. The effect on NS and 2S may be due to the Sulf enzymes influencing the biosynthetic pathway. However, whether this occurs as a result of direct interaction between the Sulfs, the nascent HS chain and/or other processing enzymes in the Golgi remains to be determined. Alternatively, these changes in NS and 2S levels could result from downstream changes in HS biosynthetic enzyme expression levels as a consequence of changes in Sulf activity.

Effect on N-sulphate distribution and transition zones - Previous *in vitro* analysis using QSulfs indicated that these enzymes preferentially remove 6S from the tri-sulphated IdoA(2S)-GlcNS(6S) disaccharide, and have no activity outside of the highly sulphated S-domains [14]. In order to analyse the domain specificity of the mammalian Sulfs, low pH nitrous acid and heparinase III depolymerisation were used to isolate and analyse the respective S-domains, non-sulphated domains and transition zones which make up the HS chain [14, 24]. HS from all cell populations was cleaved at GlcNS residues using low pH nitrous acid [27]. We compared the profiles of the resulting oligosaccharides on a Bio-Gel P10 column to determine the proportion of GlcNS-containing disaccharides within the chains (Figure 2), and to additionally provide information on domain organization (see Figure 3A). Regions of contiguous N-sulphated disaccharides (S domains) will be depolymerised to disaccharides (dp2; where dp = degree of depolymerisation) with regions of alternating GlcNS and GlcNAc residues (transition zones) generating tetrasaccharides (dp4). All profiles (Figure 2 left), were characteristic of a typical HS structure with N-sulphated residues occurring predominantly in S-domain clusters or in UA-GlcNS-UA-GlcNAc type transition zones. Minimal differences in overall macromolecular organization were visible between wild type and mSulf knock out cells. However, preparative fractionation using Bio-Gel P-10 and SAX-HPLC of low pH nitrous acid resistant tetrasaccharides did reveal important differences in sulphate composition of the transition zones (Figure 2 right). The transition zone derived tetrasaccharides separate into non-, mono- and di-sulphated species, with the variation primarily due to the addition of 6S, as these regions typically contain little 2S [6]. By comparing the contribution of each of these species we could demonstrate that there is a significant increase in 6S in the transition zones of all mSulf knock out HS, predominantly observed as an increase in mono-sulphated tetrasaccharides, while in the *mSulf1^{-/-}/2^{-/-}* HS there was a significant increase in both mono- and di-sulphated species (Figure 2 bottom).

Effect on S domain organization and composition - Heparinase III excises the S-domains in HS by specific scission of the non-sulphated regions and transition zones (see diagram in Figure 3A) [24]. Following heparinase III digestion and subsequent fractionation of the resultant oligosaccharides by Bio-Gel P-10 (Figure 3B) we observed that, similar to the nitrous acid fractionation, the overall chain macromolecular organization was conserved between the HS types (not shown). Each of the size-defined peaks were isolated separately and re-fractionated using SAX-HPLC. For tetrasaccharides and longer oligosaccharides we took advantage of a

previous study in which heparinase III digestion was used to isolate S-domains from 3T3 HS prior to sequence analysis [24]. By comparing the profiles generated in this study with those from the 3T3 HS we were able to confidently identify many of the oligosaccharides generated. Where possible, peak assignments were confirmed by isolation and disaccharide compositional analysis.

Disaccharide analysis - The disaccharide peak generated by heparinase III contained three species corresponding to UA-GlcNAc, UA-GlcNS and UA-GlcNAc(6S). These disaccharides are typically restricted to the non-sulphated and transition regions of the HS chain, confirming heparinase III enzyme specificity. In comparison to wild type HS, a significant two fold increase in UA-GlcNAc(6S) residues ($p \leq 0.01$) was seen in *mSulf1*^{-/-} material (Figure 3C, Table 2). Compensatory decreases in the non 6-O-sulphated disaccharide UA-GlcNAc were observed balancing this increase in UA-GlcNAc(6S). A similar decrease in UA-GlcNAc residues was also seen in *mSulf2*^{-/-} material, although only a 40% increase in 6-O-sulphated UA-GlcNAc(6S) residues was apparent. *mSulf1*^{-/-/2}^{-/-} material also showed a significant (60%) increase in UA-GlcNAc(6S) when compared to the wild type control. Thus, as verified by the independent nitrous acid mediated domain analysis (see above), both mSulf1 and to a lesser extent mSulf2 are active 6-O-endosulphatases within the non-sulphated and transition domains.

Tetrasaccharide analysis – Only one major tetrasaccharide species was visible in all MEF HS types following separation by SAX-HPLC (data not shown). This tetrasaccharide corresponds to ΔUA-GlcNS-IdoA(2S)-GlcNAc, confirmed by disaccharide analysis.

Hexasaccharide analysis – Eight major peaks were detected in all heparinase III derived hexasaccharides (dp6s), labelled a-h (Figure 3D). These species fall into two groups, those that are 6S deficient (6a-6c) and those with 6S (6d-6h). Peaks a-d have previously been sequenced [24], and are identified as shown in Figure 3D. Hexasaccharides e-h have an unknown sequence, however the peaks form a repeating pattern with a, b and c anticipated to have the same relationship to each other as d, e and f, etc. We could therefore predict the sequences of these species. Compared to wild type, *mSulf1*^{-/-} cell extract HS contains fewer lower sulphated sequences (peaks a-c), whereas hexasaccharides containing one or more 6-O-sulphated glucosamine residue are enriched (peaks d-h) (Figure 3D). A 53% decrease in peak a was seen in *mSulf1*^{-/-} HS, consistent with a 26% and 27% increase in peaks d and g which are modifications of a, to contain either one or two 6S glucosamine residues, respectively. The *mSulf2*^{-/-} profiles indicate little difference in the sulphated regions compared to wild type, where the only

consistent difference was an 18% increase in peak d, containing one 6-O-sulphated glucosamine residue. Comparison of wild type and *mSulf1*^{-/-}/*2*^{-/-} hexasaccharides extended the trend established in the *mSulf1*^{-/-} material, showing a marked increase in highly sulphated hexasaccharide species. This data is thus comparable to the compositional disaccharide analysis whereby distinct differences were detected between the various MEF cells in UA-GlcNS(6S) and UA(2S)-GlcNS(6S) residues contained within the S-domains (Table 1).

Octasaccharide analysis - As observed previously, the complexity of the S-domain SAX-HPLC profiles increased with increasing length [24]. Numerous species of octasaccharide (dp8) were visible, denoted a-i (Figure 3E). Some of these sequences have been previously characterised [24], however oligosaccharide peaks labelled g-i are of unknown composition, and are likely to contain more than one octasaccharide species per peak, an observation supported by subsequent analytical work [28]. *mSulf1*^{-/-} material contained clearly reduced levels of species a-c, representing S-domain regions devoid of 6S (Figure 3E). However *mSulf1*^{-/-} material was enriched in species which elute at higher salt concentrations from the column, most noticeably in octasaccharides f-i, with a 40% total increase in these saccharides compared to wild type. Again, the trends observed for *mSulf1*^{-/-} material was amplified when comparing immortalized wild type and *mSulf1*^{-/-}/*2*^{-/-} octasaccharides (Figure 3E).

Overall, the analyses of heparinase III generated hexa- and octasaccharides demonstrate that there is a clear increase in 6S in *mSulf1*^{-/-} and *mSulf1*^{-/-}/*2*^{-/-} material observed in all sizes of S-domain studied. *mSulf2*^{-/-} HS however, shows an increase in 6S almost exclusively within the non-sulphated and transition zones. Thus, the *mSulf2* knock out primarily becomes manifest outside the S-domains. Importantly, this observation contrasts with previous studies on the avian *Sulf1* and *Sulf2* orthologs where activity was restricted to within the S-domains. Specific analysis of the longer sulphated S-domains released by heparinase III as hexa- (dp6) and octasaccharides (dp8) was made possible by incorporation of data from previous studies, in which we have sequenced many of these sub-species [24]. This demonstrated clear differences in the effect of each *mSulf* knock out on S-domain sulphation patterning. As shown in Figure 3 D/E, *mSulf1*^{-/-} HS contained a greater proportion of dp6s with either one (6d-f) or two (6g-h) 6S groups; a corresponding decrease in the non-6S species (6a-c) was observed. There was also some indication that *mSulf1* activity may be favoured on adjacent GlcNS(6S) residues as the increase in species 6g containing this pattern, was greater than that seen in 6d, containing only one GlcNS(6S) residue. *mSulf1*^{-/-}/*2*^{-/-} HS-derived S-domain oligosaccharides were similar to, but

more extreme than those seen in the *mSulf1*^{-/-} HS. This detailed domain specific HS analysis provides the molecular basis needed to gain insight into the effect of dynamic changes in 6S on the biological phenotypes of the mSulf knock out mice, which are currently being characterised.

Regulation underlying 6S patterning - We were interested in a possible co-regulation of *mSulf1* and *mSulf2* at the level of gene expression. Real time PCR analysis identified an up-regulation of *mSulf1* expression in the *mSulf2*^{-/-} MEFs (Figure 4, *mSulf1* increased by 4.3 fold in *mSulf2*^{-/-} cells), which was confirmed by Northern analysis (Figure 1C). This compensatory increase of *mSulf1* in *mSulf2*^{-/-} MEFs is in good agreement with our disaccharide data where *mSulf2*^{-/-} material showed a surprising decrease in S-domain related 6S disaccharides (UA-GlcNS(6S), UA(2S)-GlcNS(6S)), and where the effect of *mSulf1*^{-/-}/*2*^{-/-} dual knock out was in excess of that suggested by either single knock out alone.

This differential activity of mSulf1 and mSulf2 in the mSulf knock out MEFs may have important biological implications. Indeed it is important to note that although no mouse 6-O-sulphotransferase knock outs have yet been published; *in vitro* experiments suggest that individual isoforms are non-specific and complementary in their sites of action [29, 30]. Therefore the predominant control of 6S patterning as seen by binding ligands is probably due to mSulf activity. How mSulf activity is dynamically coupled to generate specific sulphation patterns is likely to be critical for understanding how changes in HS structure are generated to direct cell signalling events during development and disease.

mSulf activity alters surface epitopes recognized by HS-specific antibodies – Methods to quickly and non-destructively analyse cell-surface HS sulphation patterns could significantly improve our ability to screen for sulphation state changes linked with developmental processes and disease. To approach this issue we have recently developed a method that is based on the use of a panel of phage-display derived antibodies which have specificity for a variety of saccharide patterns within HS. The ability of these antibodies to recognise specific native HS structures (some of which have recently been defined) can provide a ‘fingerprint’ of HS epitope expression on a cell [31]. When this panel of antibodies was screened against immortalised knock out and wild type cells, we found that for some of the antibodies there was little change in binding, for others the binding was decreased in the knock outs and for one antibody, RB4EA-12, binding was increased, particularly for the *mSulf1*^{-/-}/*2*^{-/-} line (Figure 5). This differential binding

behaviour supports biochemical analyses, as RB4EA-12 has previously been shown to have a specific requirement for 6S [32, 33]. Furthermore, antibodies EV3C3 and HS4E4 which showed reduced binding to mSulf knock out MEFs are known to be inhibited by 6S [32]. Therefore, in keeping with the documented complexity of Sulf activity on HS-ligand binding, we found that depending on the antibody used, loss of mSulf activity had a negative effect (i.e. less binding), no effect or a positive effect on antibody binding (Figure 5) demonstrating the potential for differential regulation of ligand-binding epitopes within HS by altered mSulf activity. This further indicates that mSulf activity can simultaneously influence multiple ligand-binding events, likely through induced changes in HS structure [34]. In view of the paucity of detailed 3D information on HS motifs, this panel of antibodies provides a useful screening tool for evaluating these changes.

Loss of mSulf activity increases the mitogenic response of MEFs - The antibody study above suggested that ligand-binding may be affected by mSulf activity. However, the regulatory activity of HS for its many interacting factors is more complex than can be explained by binding affinity alone [24] and indeed, in some instances high affinity binding is inhibitory for activity. mSulf activity has previously been linked with the activity of a number of HS-dependent growth factors and morphogens, including the multi-functional FGF2 [15]. We therefore employed a simple proliferation assay using primary MEFs to ascertain if there was any differential activity between the mSulf mutant lines. MEF cell cultures have previously been shown to be suitable for these studies [22]. Results demonstrate a significant increase in proliferation of both single mSulf knock out cells, particularly for *mSulf1*^{-/-} in which FGF2 induced a three-fold increase in proliferation compared to wild type (Figure 6). No mitogenic response was observed with HGF in any of the MEFs tested, in agreement with previous studies (C. Merry, unpublished).

Conclusions

In conclusion, loss of mSulf1 or mSulf2 activity in MEFs is associated with increases in HS 6S. Notably, the domain-specific pattern of this increase, its influence on other sulphation activity and the potential effect this has on ligand binding patterns (as revealed by antibody reactivities) are different for the two enzymes. Additionally, this study presents strong evidence to suggest that mSulf1 and mSulf2 act cooperatively and are the major regulators of 6S patterns within HS (Figure 7). The focus of future study will be the analysis of the knock out mice themselves,

particularly to characterise the ability of the mSulfs to regulate specific developmental patterning events and tumourigenesis *in vivo*. Based on this characterisation of mSulf knock out MEFs we would predict many HS-ligand interactions will be affected by the structural alterations, particularly for the *mSulf1*^{-/-}/*2*^{-/-} mouse.

FOOTNOTES

Acknowledgments - We would like to thank Nicole Tasch, Ellen Eckermann-Felkl, Martina Balleininger and Annegret Schneemann for excellent technical assistance, Peter Gruss for providing embryonic stem cells and Paul Saftig for his advice in knock out mouse generation. This work was supported by the Deutsche Forschungsgemeinschaft, the Fonds der Chemischen Industrie, Cancer Research UK and the British Council UK-Netherlands Partnership Programme in Science.

Abbreviations - The abbreviations used are: HSPG, heparan sulfate proteoglycan; HS, heparan sulfate; FGF, fibroblast growth factor; HGF/SF, hepatocyte growth factor/scatter factor; VEGF, vascular endothelial growth factor; HB-EGF, heparan binding – EGF like growth factor; UA, hexuronic acid; Δ UA, delta 4,5 unsaturated hexuronic acid; GlcA, glucuronic acid; IdoA, iduronic acid; GlcNAc, N-acetylglucosamine; GlcNS, N-sulfoglucosamine; 2S and 6S, 2-*O*- and 6-*O*-sulfation, respectively; NS, N-sulphation; ERK, extracellular signal regulated kinase; SAX-HPLC, strong anion exchange high pressure liquid chromatography; MEF, mouse embryonic fibroblast.

REFERENCES

1. Bernfield, M., Gotte, M., Park, P.W., Reizes, O., Fitzgerald, M.L., Lincecum, J., and Zako, M. (1999) Functions of cell surface heparin sulphate proteoglycans. *Annu. Rev. Biochem.* **68**, 729-777
2. Rapraeger, A.C., Krufka, A., and Olwin, B.B. (1991) Requirement of heparin sulphate for bFGF-mediated fibroblast growth and myoblast differentiation. *Science* **252**, 1705-1708
3. Yayon, A., Klagsbrun, M., Esko, J.D., Leder, P., and Ornitz, D.M. (1991) Cell surface, heparin-like molecules are required for binding of basic fibroblast growth factor to its high affinity receptor. *Cell* **64**, 841-848
4. Esko, J.D. and Lindahl, U. (2001) Molecular diversity of heparin sulfate. *J. Clin. Invest.* **108**, 169-173
5. Ledin, J., Staatz, W., Li, J.P., Gotte, M., Selleck, S., Kjellen, L., and Spillmann, D. (2004) Heparan sulfate structure in mice with genetically modified heparan sulfate production. *J. Biol. Chem.* **279**, 42732-42741
6. Maccarana, M., Sakura, Y., Tawada, A., Yoshida, K., and Lindahl, U. (1996) Domain structure of heparan sulfates from bovine organs. *J. Biol. Chem.* **271**, 17804-17810
7. Pye, D.A., Vives, R.R., Hyde, P., and Gallagher, J.T. (2000) Regulation of FGF-1 mitogenic activity by heparan sulfate oligosaccharides is dependent on specific structural features: differential requirements for the modulation of FGF-1 and FGF-2. *Glycobiology* **10**, 1183-1192
8. Brickman, Y.G., Ford, M.D., Gallagher, J.T., Nurcombe, V., Bartlett, P.F., and Turnbull, J.E. (1998) Structural modification of fibroblast growth factor-binding heparin sulphate at a determinative stage of neural development. *J. Biol. Chem.* **273**, 4350-4359
9. Jayson, G.C., Vives, C., Paraskeva, C., Schofield, K., Coutts, J., Fleetwood, A., and Gallagher, J.T. (1999) Coordinated modulation of the fibroblast growth factor dual receptor mechanism during transformation from human colon adenoma to carcinoma. *Int. J. Cancer.* **82**, 298-304
10. Dhoot, G.K., Gustafsson, M.K., Ai, X., Sun, W., Standiford, D.M., and Emerson, C.P., Jr. (2001) Regulation of Wnt signalling and embryo patterning by an extracellular sulfatase. *Science* **293**, 1663-1666

11. Morimoto-Tomita, M., Uchimura, K., Werb, Z., Hemmerich, S., and Rosen, S.D. (2002) Cloning and characterization of two extracellular heparin-degrading endosulfatases in mice and humans. *J. Biol. Chem.* **277**, 49175-49185
12. Ai, X., Do, A.T., Kusche-Gullberg, M., Lindahl, U., Lu, K., and Emerson, C.P., Jr. (2006) Substrate Specificity and Domain Functions of Extracellular Heparan Sulfate 6-O-Endosulfatases, QSulf1 and QSulf2. *J. Biol. Chem.* **281**, 4969-4976
13. Ai, X., Do, A.T., Lozynska, O., Kusche-Gullberg, M., Lindahl, U., and Emerson, C.P., Jr. (2003) QSulf1 remodels the 6-O sulfation states of cell surface heparan sulfate proteoglycans to promote Wnt signaling. *J. Cell. Biol.* **162**, 341-351
14. Viviano, B.L., Paine-Saunders, S., Gasiunas, N., Gallagher, J., and Saunders, S. (2004) Domain-specific Modification of Heparan Sulfate by QSulf1 Modulates the Binding of the Bone Morphogenetic Protein Antagonist Noggin. *J. Biol. Chem.* **279**, 5604-5611
15. Wang, S., Ai, X., Freeman, S.D., Pownall, M.E., Lu, Q., Kessler, D.S., and Emerson, C.P., Jr. (2004) QSulf1, a heparan sulfate 6-O-endosulfatase, inhibits fibroblast growth factor signaling in mesoderm induction and angiogenesis. *Proc. Natl. Acad. Sci.* **101**, 4833-4838
16. Lai, J., Chien, J., Staub, J., Avula, R., Greene, E.L., Matthews, T.A., Smith, D.I., Kaufmann, S.H., Roberts, L.R., and Shridhar, V. (2003) Loss of HSulf-1 up regulates heparin-binding growth factor signaling in cancer. *J. Biol. Chem.* **278**, 23107-23117
17. Li, J., Kleeff, J., Abiatari, I., Kayed, H., Giese, N.A., Felix, K., Giese, T., Buchler, M.W., and Friess, H. (2005) Enhanced levels of HSulf-1 interfere with heparin-binding growth factor signaling in pancreatic cancer. *Mol. Cancer* **4**, 14
18. Morimoto-Tomita, M., Uchimura, K., Bistrup, A., Lum, D.H., Egeblad, M., Boudreau, N., Werb, Z., and Rosen, S.D. (2005) Sulf-2, a proangiogenic heparan sulfate endosulfatase, is up regulated in breast cancer. *Neoplasia* **7**, 1001-1010
19. Lai, J.P., Chien, J., Strome, S.E., Staub, J., Montoya, D.P., Greene, E.L., Smith, D.I., Roberts, L.R., and Shridhar, V. (2004) HSulf-1 modulates HGF-mediated tumor cell invasion and signaling in head and neck squamous carcinoma. *Oncogene* **23**, 1439-1447
20. Lai, J.P., Chien, J.R., Moser, D.R., Staub, J.K., Aderca, I., Montoya, D.P., Matthews, T.A., Nagorney, D.M., Cunningham, J.M., Smith, D.I., Greene, E.L., Shridhar, V., and Roberts, L.R. (2004) HSulf-1 Sulfatase promotes apoptosis of hepatocellular cancer cells by decreasing heparin-binding growth factor signaling. *Gastroenterology* **126**, 231-248

21. Uchimura, K., Morimoto-Tomita, M., Bistrup, A., Li, J., Lyon, M., Gallagher, J., Werb, Z., and Rosen, S.D. (2006) HSulf-2, an extracellular endoglucosamine-6-sulfatase, selectively mobilizes heparin-bound growth factors and chemokines: effects on VEGF, FGF-1, and SDF-1. *BMC Biochem.* **7**, 2
22. Merry, C.L., Bullock, S.L., Swan, D.C., Backen, A.C., Lyon, M., Beddington, R.S., Wilson, V.A., and Gallagher, J.T. (2001) The molecular phenotype of heparan sulfate in the Hs2st-/- mutant mouse *J. Biol. Chem.* **276**, 35429-35434
23. Schuermann M. (1990) An expression vector system for stable expression of oncogenes. *Nucleic Acids Res.* **18**, 4945-4946
24. Merry, C.L.R., Lyon, M., Deakin, J.A., Hopwood, J.J., and Gallagher, J.T. (1999) Highly sensitive sequencing of the Sulfated Domains of Heparan Sulphate. *J. Biol. Chem.*, **274**, 18455-18462
25. Mouritzen, P., Nielsen, P.S., Jacobsen, N., Noerholm, M., Lomholt, C., Pfundheller, H.M., Ramsing, N.B., Kauppinen, S., Tolstrup, N. (2004) The Probe Library: Expression profiling of 99% of all human genes using only 90 dual labeled real time PCR probes. *BioTechniques* **37**, 492-495
26. Livak, K.L., and Schmittgen, T.D. (2001) Analysis of relative gene expression data using real-time quantitative PCR and the 2(-delta delta C(T)) method. *Methods* **25**, 402-408
27. Shively, J.E., and Conrad, H.E. (1976) Formation of anhydrosugars in the chemical depolymerization of heparin. *Biochemistry* **15**, 3932-3942
28. Robinson, C.J., Mulloy, B., Gallagher, J.T. and Stringer, S.E. (2006) VEGF165-binding sites within heparan sulfate encompass two highly sulfated domains and can be liberated by K5 lyase. *J. Biol. Chem.* **281**, 1731-1740
29. Do, A.T., Smeds, E., Spillmann, D., and Kusche-Gullberg, M. (2005) Overexpression of heparan sulfate 6-O-sulfotransferases in human embryonic kidney 293 cells results in increased N-acetylglucosaminyl 6-O-sulfation. *J. Biol. Chem.* **9**, 5348-5356
30. Smeds, E., Habuchi, H., Do, A.T., Hjertson, E., Grundberg, H., Kimata, K., Lindahl, U., and Kusche-Gullberg, M. (2003) Substrate specificities of mouse heparan sulphate glucosaminyl 6-O-sulphotransferases. *Biochem. J.* **372**, 371-380
31. van Kuppevelt, T.H., Dennissen, M.A., van Venrooij, W.J., Hoet, R.M., and Veerkamp, J.H. (1998) Generation and application of type-specific anti-heparan sulfate antibodies using

- phage display technology. Further evidence for heparan sulfate heterogeneity in the kidney. *J. Biol. Chem.* **273**, 12960-12966
32. Dennissen, M.A., Jenniskens, G.J., Pieffers, M., Versteeg, E.M., Petitou, M., Veerkamp, J.H., and van Kuppevelt, T.H. (2002) Large, tissue-regulated domain diversity of heparan sulfates demonstrated by phage display antibodies. *J. Biol. Chem.* **277**, 10982-10986
33. Jenniskens, G.J., Oosterhof, A., Brandwijk, R., Veerkamp, J.H., and van Kuppevelt, T.H. (2000) Heparan sulfate heterogeneity in skeletal muscle basal lamina: demonstration by phage display-derived antibodies. *J. Neurosci.* **20**, 4099-4111
34. Raman, R., Sasisekharan, V., and Sasisekharan, R. (2005) Structural insights into biological roles of protein-glycosaminoglycan interaction. *Chem. Biol.* **12**, 267-277

FIGURE LEGENDS

Figure 1. Targeted disruption of murine *Sulf1* and *Sulf2*.

A, B: Schematic representation of the murine *Sulf1* (*A*) and *Sulf2* (*B*) loci in the area of the targeted exon 2 (*A*) and exon 1 (*B*), respectively. The three illustrations show the wild type locus (top), the targeting vector (middle) and the recombined allele (bottom). Recombined alleles carry the neomycin resistance cassette inserted into the *Bsa*AI site of *mSulf1* exon 2 (*A*) and the *Bse*RI site of *mSulf2* exon 1 (*B*), respectively. The location of the 5' and 3' external probes used for Southern hybridization and the relevant restriction sites and resulting fragments are indicated. Successful and specific germline targeting was confirmed by Southern blotting of *Stu*I- or *Sac*I-digested genomic DNA using the indicated external probes (see blot insets in *A* and *B*, respectively). Results were confirmed by independent external probes detecting the indicated 3.9 kb fragment in *Bam*HI-digested DNA (*SULF1, A*) and the 5.2 kb fragment in *Kpn*I/*Xho*I-digested DNA (*SULF2, B*) (data not shown). *C:* Northern blot analysis of total RNA (10 µg) from wild type, *mSulf1*^{-/-} and *mSulf2*^{-/-} MEFs, using probes for *mSulf2*, *mSulf1* and *β-actin*.

Figure 2 Low pH nitrous acid depolymerisation of cell extract HS.

Following treatment with low pH nitrous acid, HS was fractionated by Bio-Gel P-10 (left hand panel) to separate size-defined oligosaccharides (dp2, dp4 etc. where dp=degree of depolymerisation e.g. dp2=disaccharide). The proportion of counts in each sized peak was found to be very similar between the samples - dp2=14-15%, dp4 28-30% (primary cells) and dp2=22%, dp4=31-32% (immortalised cells). Tetrasaccharides (from UA-GlcNAc-UA-GlcNS regions of the chains) were further fractionated by SAX-HPLC (right hand panels) into di-, mono- and non-sulphated species. These were then quantified (bottom panels) for the primary MEFs: wild type (black bars), *mSulf1*^{-/-} (white bars) and *mSulf2*^{-/-} (check bars); and the immortalised MEF lines: wild type (downwards diagonal bars) and *mSulf1*^{-/-}/*2*^{-/-} (upwards diagonal bars). All profiles are representative of at least three separate fractionations.

Figure 3. Sulphated Domain analysis of cell extract HS.

HS was digested with heparinase III. *A:* Site of action of heparinase III (white arrow) and low pH nitrous acid (black arrows). Non-N-sulphated domains (black box), transition zone NS/NAC (white box) and S-domains (striped box) are indicated. *B:* Typical HS profile following

heparinase III digestion and separation on a Bio-Gel P-10 column. Di- tetra-, hexa- and octasaccharide fractions indicated were pooled and further fractionated using SAX-HPLC. Three disaccharide species were identified (C), eight hexasaccharide species (D) and a complex range of octasaccharide species, some of which were pooled as indicated (E). Many of the oligosaccharides could be identified by comparison of elution position with that of known standards and where possible, by disaccharide analysis. Data from at least 3 profiles was quantitated to generate the bar charts shown: primary MEFs; wild type (black bars), *mSulf1*^{-/-} (white bars) and *mSulf2*^{-/-} (check bars); and the immortalised MEF lines: wild type (downwards diagonal bars) and *mSulf1*^{-/-/2}^{-/-} (upwards diagonal bars).

Figure 4. Real-time PCR analysis of the expression of mSulf enzymes in knock out MEFs.

An average of the two house-keeping genes L19 and EEFIG was used to normalise the cDNAs of each sample relative to each other. The fold change for *mSulf1*^{-/-} and *mSulf2*^{-/-} MEFs was calculated relative to the primary MEF wild type control. Values for *mSulf1*^{-/-/2}^{-/-} MEFs were calculated relative to an immortalised wild type control. A fold change greater than 2 was judged to be significant (dotted line). *mSulf1*^{-/-} (clear bars), *mSulf2*^{-/-} (check bars) and *mSulf1*^{-/-/2}^{-/-} (upwards diagonal bars). *mSulf1* expression was reduced 10 fold in the *mSulf1*^{-/-} cells, increased 4.3 fold in the *mSulf2*^{-/-} cells and decreased 18 fold in the *mSulf1*^{-/-/2}^{-/-} cells. *mSulf2* expression was decreased 2.2 fold in the *mSulf1*^{-/-} cells, decreased 77 fold in the *mSulf2*^{-/-} cells and decreased 19 fold in the *mSulf1*^{-/-/2}^{-/-} cells.

Figure 5. HS epitope-specific ScFv antibodies show altered cell binding characteristics for mSulf knock out MEFs.

Immortalised wild type (black line), *mSulf1*^{-/-} (green line), *mSulf2*^{-/-} (blue line) and *mSulf1*^{-/-/2}^{-/-} (purple line) MEFs were incubated with a panel of HS sequence-specific ScFv antibodies. These were then analysed by FACS to demonstrate a shift in binding profile for each of the MEFs with the various antibodies. The profiles shown for three of the antibodies, as indicated, are representative of at least three different experiments. Control profiles (using secondary antibody alone) are shown as the filled red profiles.

Figure 6. Loss of mSulf activity increases the mitogenic response of MEFs to FGF2.

Primary MEFs were allowed to quiesce in serum free medium prior to induction with either FGF2 or HGF. *mSulf1*^{-/-} (white bars) and *mSulf2*^{-/-} (check bars) cells showed a markedly increased mitogenic response to FGF2 as compared to wild type (upwards diagonal bars). Exposure to HGF resulted in no mitogenic response in all MEFs.

Figure 7. Sulfs are major regulators of 6-O-sulphation within HS.

The addition of 6S to the nascent HS chain within the Golgi is mediated by a family of 6-O-sulphotransferases. Our data suggests that these modifications are fairly extensive throughout the chain (leading to ~40% of disaccharides containing 6S groups). It is the activity of the mSulf enzymes that reduces this level to the ~15% which is found in HS prepared from tissues and which finalises the complex sulphate patterning observed on mature HS chains.

TABLES

Table 1: Disaccharide composition and overall sulphation of knock out HS from cell extract fractions. Im. = immortalised

	WT (%)	<i>mSulf1</i> ^{-/-} (%)	<i>mSulf2</i> ^{-/-} (%)	Im. WT (%)	Im. <i>mSulf1</i> ^{-/-} / <i>2</i> ^{-/-} (%)
UA-GlcNAc	49.5	49.6	52.7	45.4	37.5
UA-GlcNS	21.5	20.0	22.2	23.5	20.3
UA-GlcNAc(6S)	5.9	11.1	7.7	7.5	12.6
UA(2S)-GlcNAc	2.7	1.7	1.3	1.4	1.0
UA-GlcNS(6S)	3.7	5.8	3.1	5.1	13.7
UA(2S)-GlcNS	10.9	4.5	8.8	10.4	1.8
UA(2S)- GlcNS(6S)	5.8	7.4	4.2	6.8	13.1
Total NAc	58.1	62.4	61.8	54.2	51.1
Total NS	41.9	37.6	38.2	45.8	48.9
Total 2S	19.3	13.5	14.3	18.5	15.9
Total 6S	15.4	24.2	15.0	19.4	39.3

Table 2: **Relative amounts of heparinase III generated disaccharides.** Im.=immortalised

	WT (%)	<i>mSulf1</i> ^{-/-} (%)	<i>mSulf2</i> ^{-/-} (%)	Im. WT (%)	Im. <i>mSulf1</i> ^{-/-} / <i>2</i> ^{-/-} (%)
UA-GlcNAc	75.5	69.7	70.5	68.1	66.1
UA-GlcNS	19.9	21.4	23.0	24.7	22.4
UA-GlcNAc(6S)	4.7	9.0	6.5	7.2	11.5

Figure 1

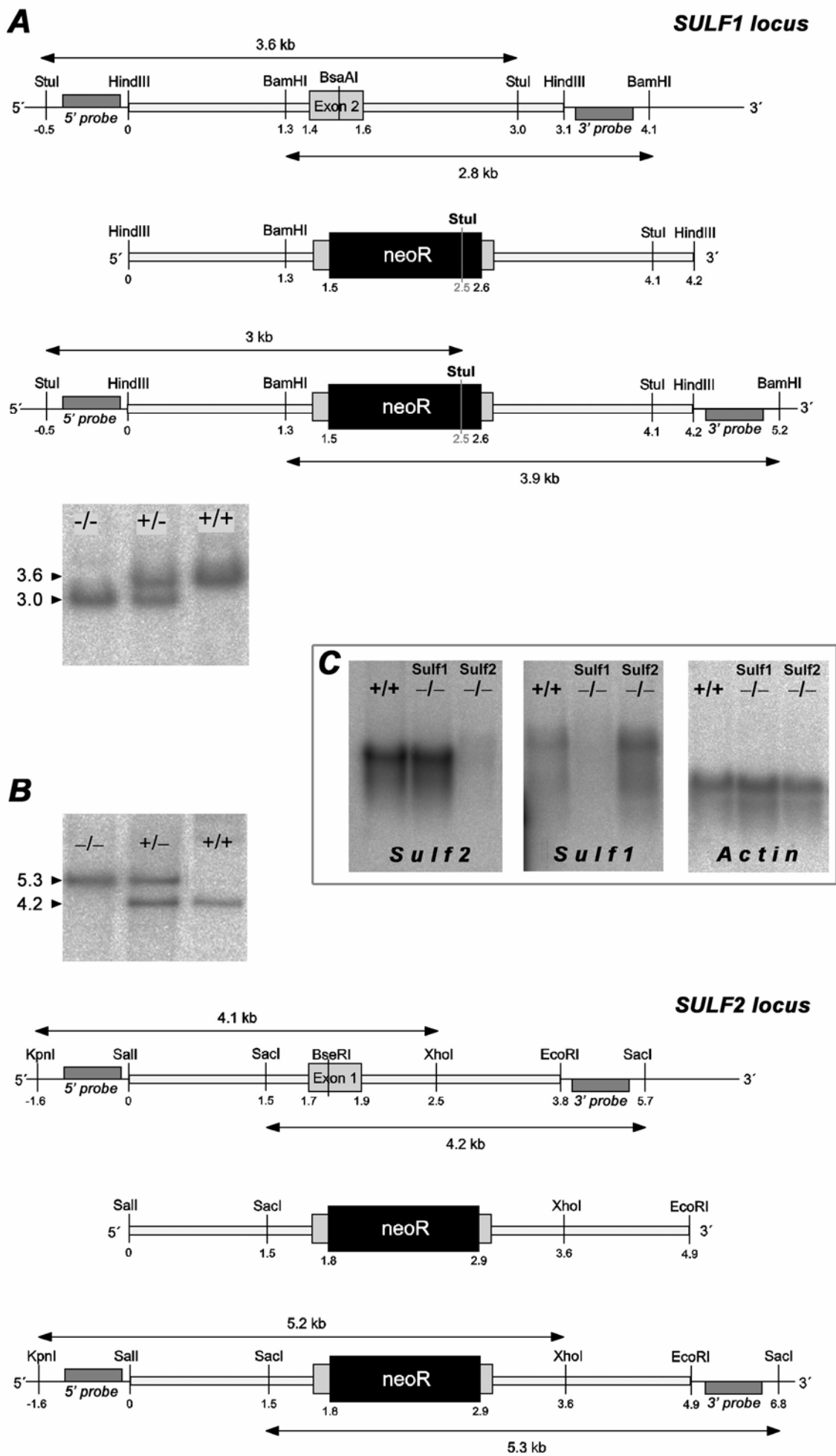


Figure 2

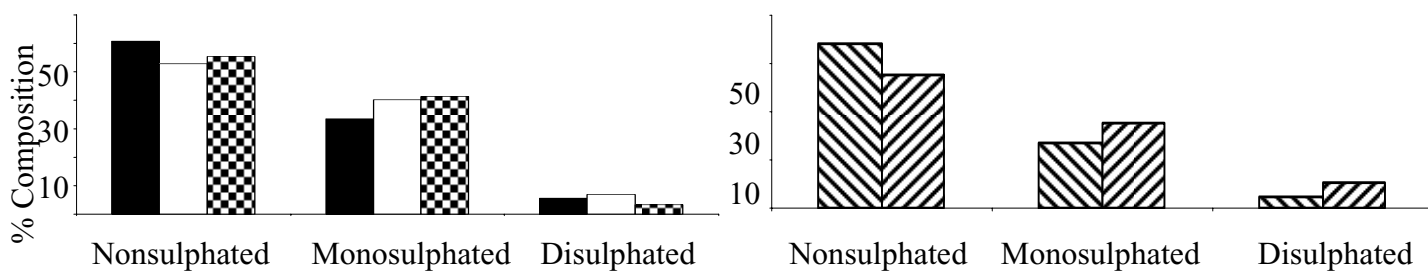
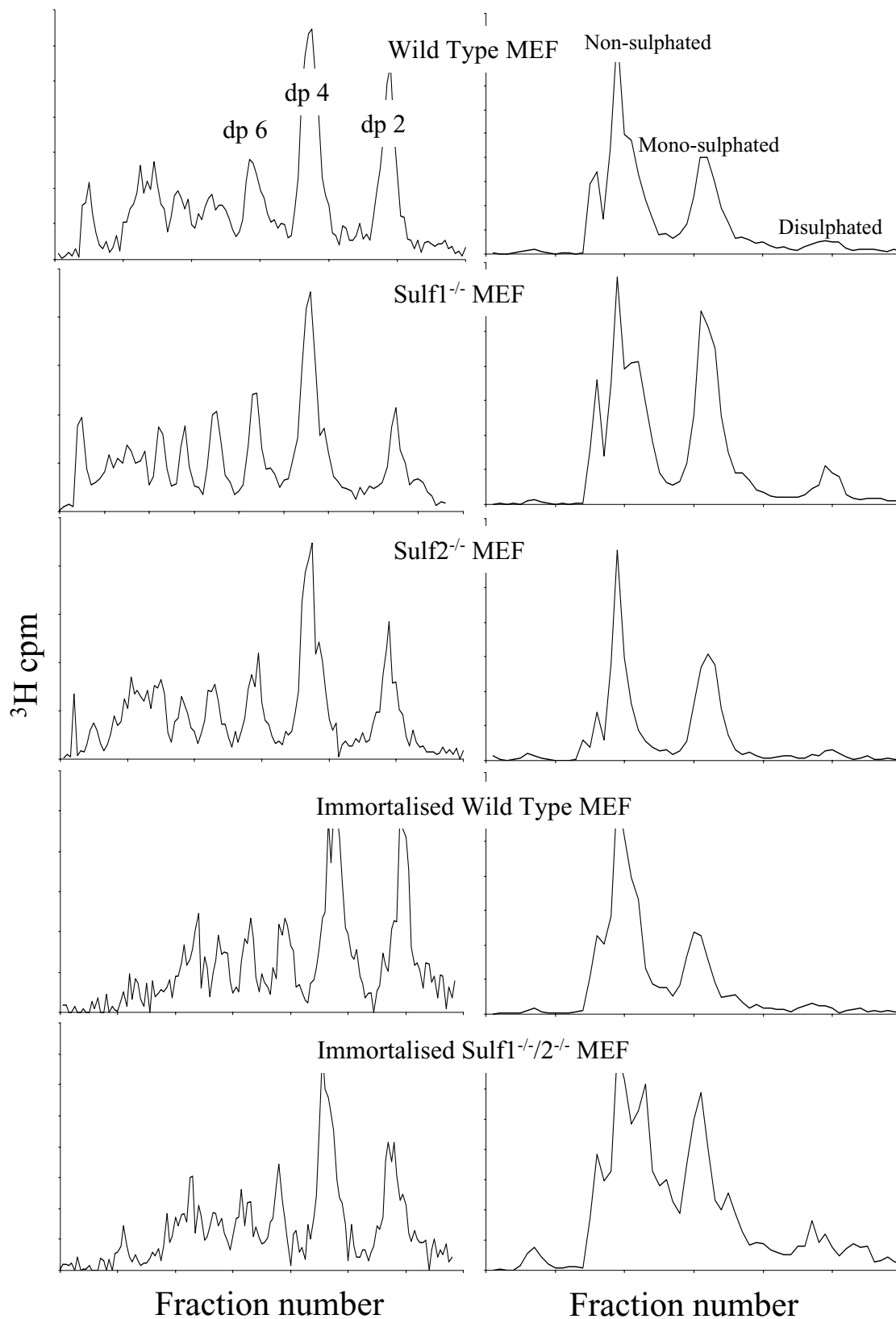


Figure 3

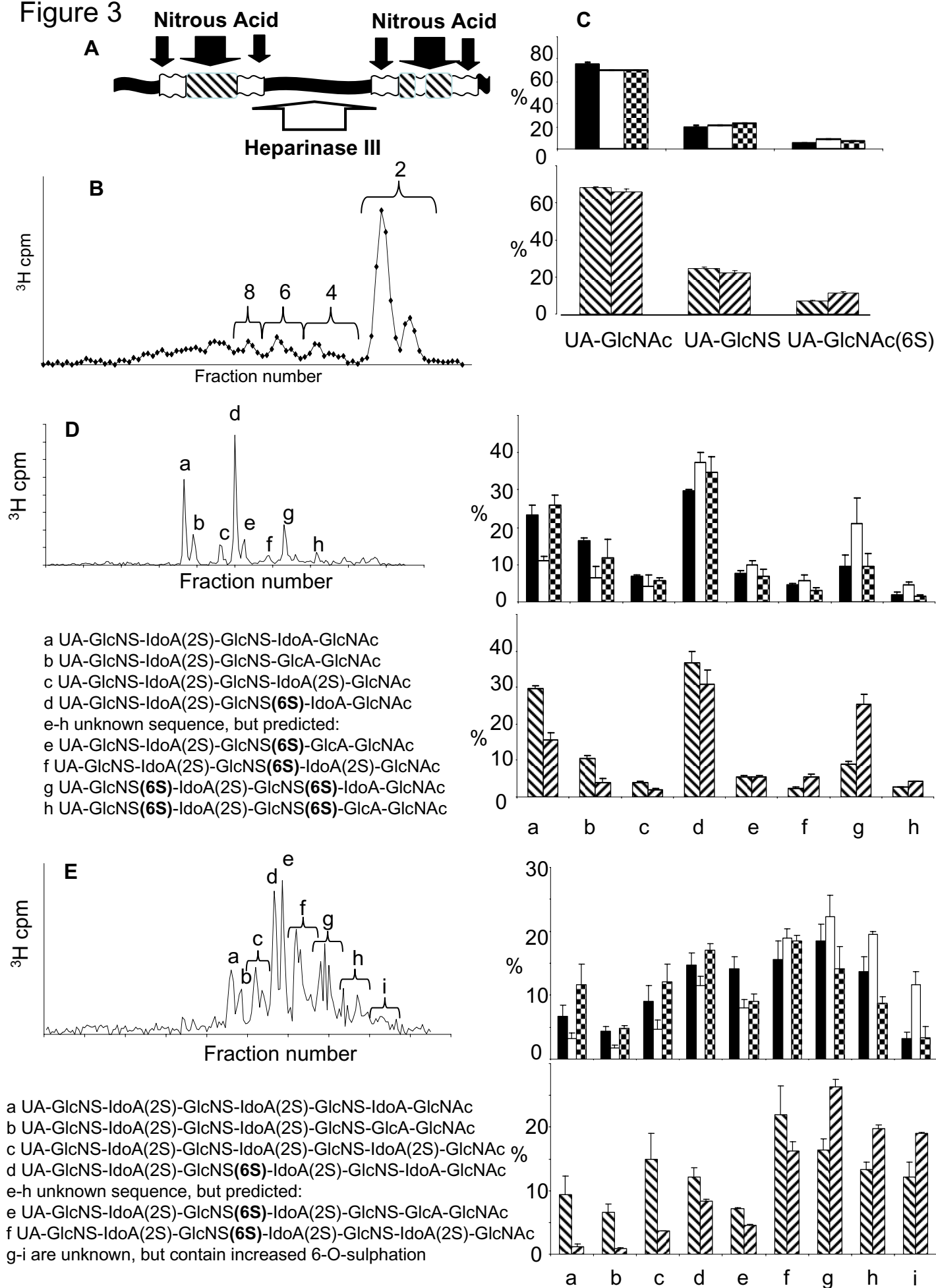


Figure 4

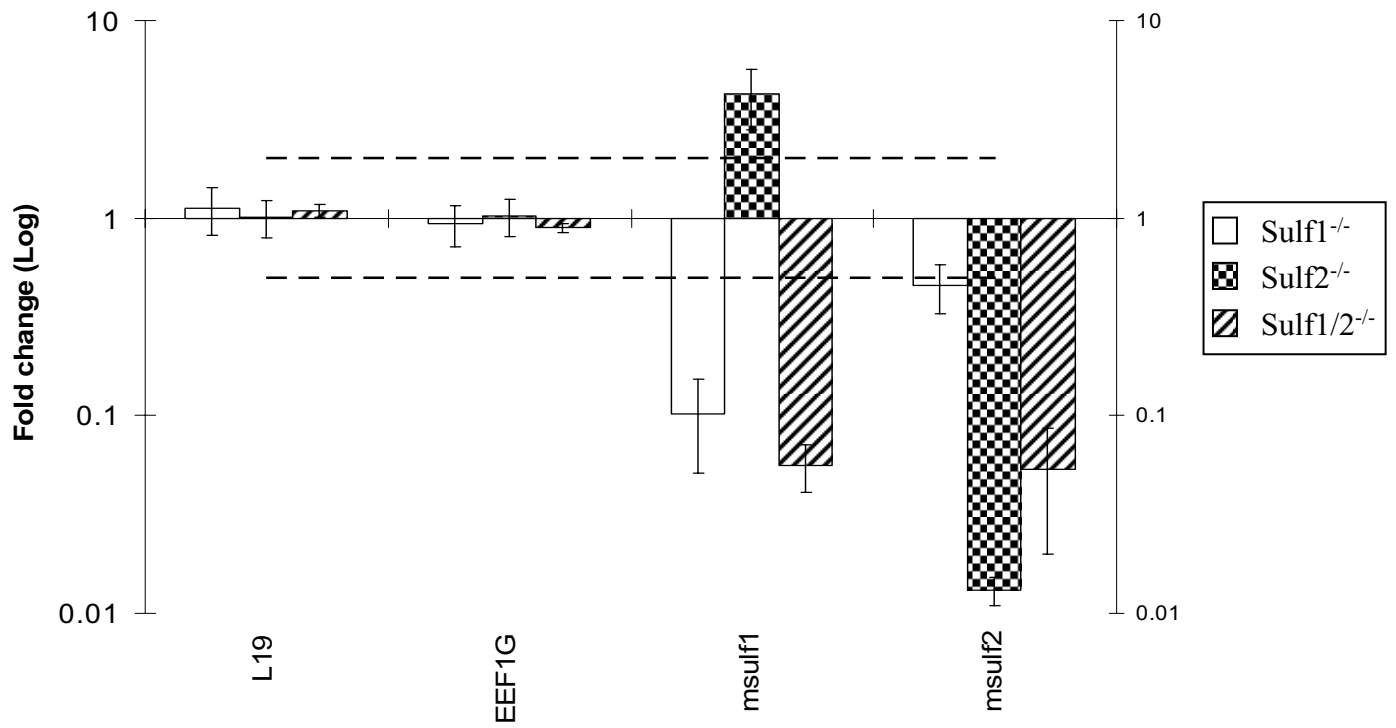


Figure 5

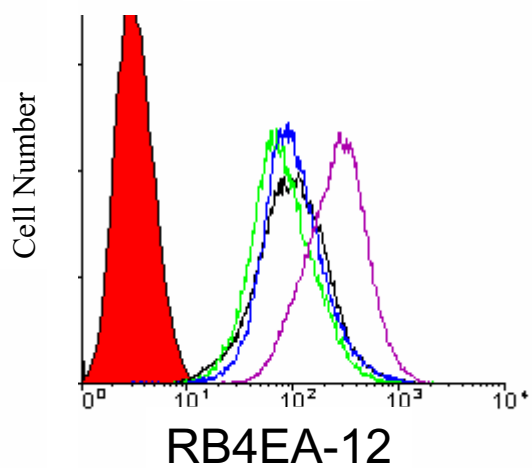
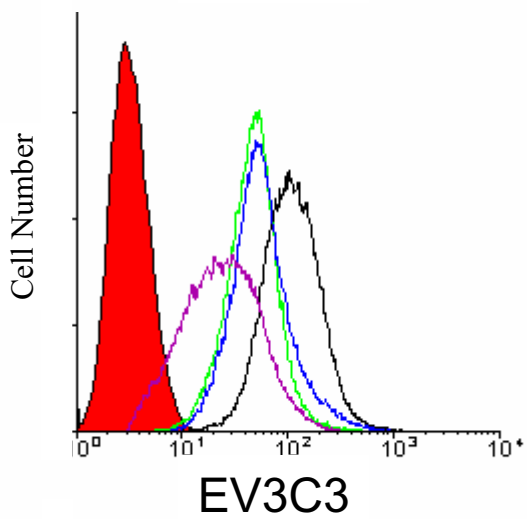
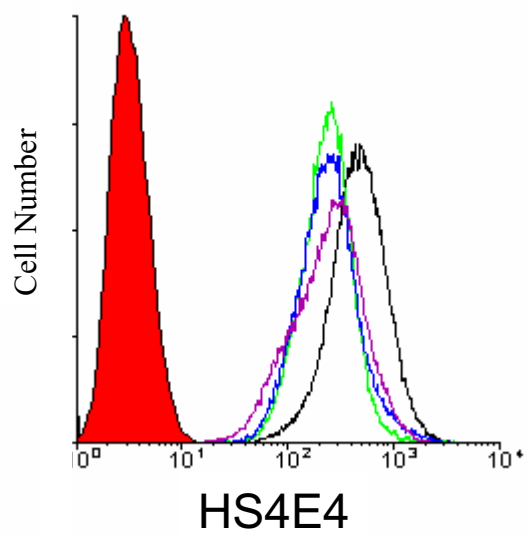


Figure 6

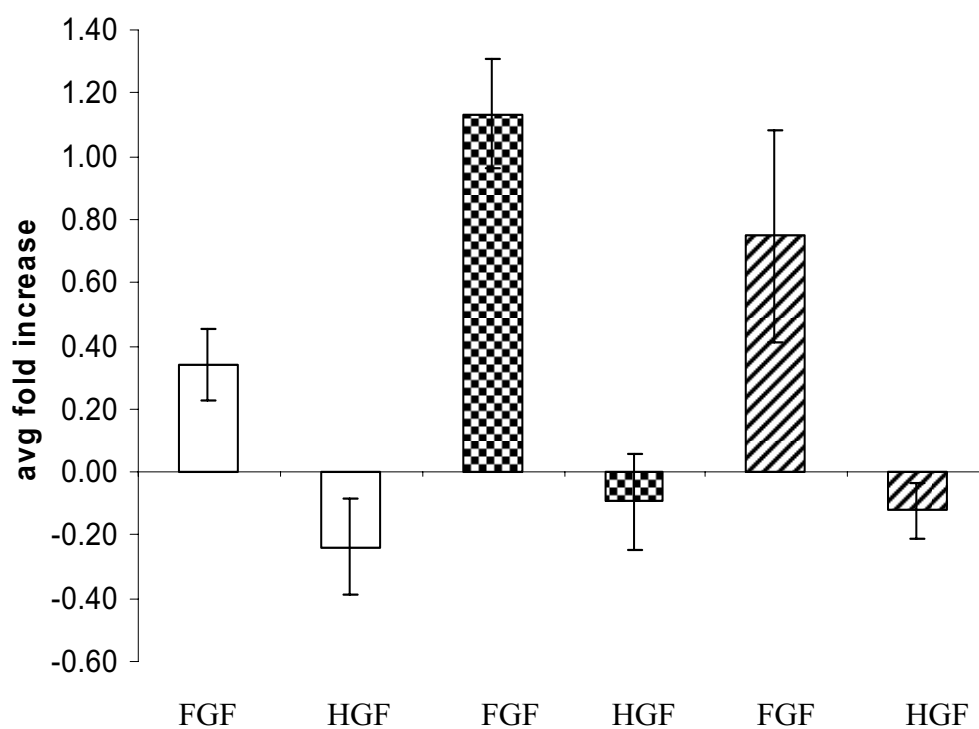


Figure 7

